



HAL
open science

Validation of a novel finite-element model for evaluating patellofemoral forces and stress during squatting after posterior-stabilized total knee arthroplasty

Salah Mebarki, Franck Jourdan, François Canovas, Etienne Malachanne,
Louis Dagneaux

► To cite this version:

Salah Mebarki, Franck Jourdan, François Canovas, Etienne Malachanne, Louis Dagneaux. Validation of a novel finite-element model for evaluating patellofemoral forces and stress during squatting after posterior-stabilized total knee arthroplasty. *Orthopaedics & Traumatology: Surgery & Research*, 2022, pp.103519. 10.1016/j.otsr.2022.103519 . hal-03934907

HAL Id: hal-03934907

<https://hal.science/hal-03934907v1>

Submitted on 11 Jan 2023

HAL is a multi-disciplinary open access archive for the deposit and dissemination of scientific research documents, whether they are published or not. The documents may come from teaching and research institutions in France or abroad, or from public or private research centers.

L'archive ouverte pluridisciplinaire **HAL**, est destinée au dépôt et à la diffusion de documents scientifiques de niveau recherche, publiés ou non, émanant des établissements d'enseignement et de recherche français ou étrangers, des laboratoires publics ou privés.

Validation of a novel finite-element model for evaluating patellofemoral forces and stress during squatting after posterior-stabilized total knee arthroplasty

Salah Mebarki^a, Franck Jourdan^a, François Canovas^b, Etienne Malachanne^a,
Louis Dagneaux^{a,b,*}

^a Laboratoire de mécanique et génie civil (LMGC), CNRS, Montpellier University of Excellence (MUSE), 860, rue de St-Priest, 34090 Montpellier, France

^b Department of Orthopaedic Surgery, Lower limb Surgery Unit, Lapeyronie University Hospital, Montpellier University, 371, avenue Gaston-Giraud, 34295 Montpellier, France

Introduction: Several studies have documented the relationship between patellofemoral pain and patient dissatisfaction after total knee arthroplasty (TKA). However, few computer simulations have been designed to evaluate the patellofemoral joint during flexion. The aim of this study was to validate a new computational simulation, driven by forces and moments, and to analyze patellofemoral reaction forces and stress under squat loading conditions after TKA implantation.

Hypothesis: This computational simulation of a squat using a model driven by forces and moments is comparable to *in vitro* and *in silico* data from the literature.

Material and methods: We developed a finite element model of the lower limb after implantation of a fixed-bearing posterior-stabilized TKA. To simulate squat loading conditions when standing on both legs, an initial load of 130 N was applied to the center of the femoral head. Quadriceps force, patellofemoral contact force and Von Mises stress on the patellar implant, tibiofemoral contact forces and pressure on the tibial insert, and post-cam contact force were evaluated from 0° to 100° of knee flexion.

Results: Quadriceps force increased during flexion, up to 6 times the applied load. Von Mises stress on patellar implant increased up to 16 MPa at 100° flexion. Tibiofemoral contact forces increased up to 415 N medially and 339 N laterally, with 64% distributed medially on the tibial insert.

Post-cam contact started slightly before 70° of flexion.

Discussion: In this simulation, tibiofemoral, patellofemoral and post-cam contact forces, and pressure distribution on the tibial insert were consistent with various published studies. This agreement suggests that computational simulation driven by forces and moments can reproduce squat loading conditions during knee flexion after TKA, without experimental kinematic data used to drive the simulation.

Conclusion: This study represents an initial step towards validating tibiofemoral and patellofemoral mechanical behavior under squat conditions, from this computational simulation driven by forces and moments. This model will help us better understand the influence of various implantation techniques on patellofemoral forces and stress during flexion.

Level of evidence: IV, biomechanical computational study.

Keywords:

Computational model
Biomechanics
Knee replacement
Alignment
Patellofemoral

1. Introduction

Undergoing total knee arthroplasty (TKA) allows patients to improve their daily activities by providing pain relief and optimized

knee range of motion in the context of severe knee osteoarthritis [1]. Nevertheless, a substantial number of patients are not satisfied after TKA [1,2]. While patellofemoral pain is one of the most common reasons for patient dissatisfaction [1–3], it remains difficult to predict clinically which patient will experience patellofemoral pain after undergoing TKA [4]. Thus, a biomechanical evaluation of the patellofemoral joint is crucial for understanding the occurrence of anterior knee pain relative to which implantation technique is used.

Abbreviations: TKA, Total Knee Arthroplasty; FEM, Finite element model; CAD, Computer Assisted Design; N, Newtons; MPa, MegaPascal.

* Corresponding author.

E-mail address: louisdagneaux@gmail.com (L. Dagneaux).

Table 1
Definitions and specific terms.

English terms	Definition
Biomechanics	Application of mechanical principles to living organisms
Force	Mechanical action resulting in the displacement, acceleration, or deformation of a solid
Moment arm	Distance from the axis of rotation to the applying point of the force
Torque	Ability of a force to rotate a solid
Loads and constraints	Forces and moments applied to the solid as external actions
(Von Mises) stress	Inner body pressure defined as the ratio between the applied force and the surface (MPa)
Contact pressure	Mechanical interaction due to contact forces between two solids (MPa)
Boundary conditions	Actions defined prior to the simulation, imposing a value on displacements or forces (ex: fixed tibial bone)
Region of interest (ROI)	Anatomical landmarks or surface on which the output data from the computational model are collected

Among the mechanical conditions studied after TKA, a squatting movement is typically used in computer simulations [5–7]. The patient’s ability to flex their knee as much as possible from an extended leg position is often considered representative of activities of daily living and correlated with clinical results [8]. An increase in patellar loads at about 60° flexion has been observed in simulations during squatting after TKA [8,9]. However, the role of tension in the patellar retinaculum is unspecified in these simulations.

Various finite element models (FEM) have been described in the literature, each having their own complexity, precision and functionality [10–13]. Some computer simulations have been proven effective at predicting the tibiofemoral loads during a squat [14], but few models have focused on evaluating the patellofemoral joint during flexion. The boundary conditions and loading conditions are very different in these various models, making them difficult to compare [15,16]. The aim of this study was to validate a new computational model driven by forces and moments and to analyze patellofemoral reaction forces and stress during squatting after TKA implantation (Table 1).

2. Materials and methods

2.1. Knee and implant geometry

Bone geometries were extracted from preoperative CT-scan slices (General Electric Healthcare, Milwaukee, WI, USA) from a

single patient with end-stage knee osteoarthritis and varus deformity, operated on for a TKA (Fig. 1). Three-dimensional (3D) reconstructions were completed using open-source 3D image processing software (3D Slicer, version 4.11) based on manual segmentation of the femur, tibia, fibula and patella. The final parametric model was exported in STL format and included the volumes of each bone. The mechanical and anatomical axes and the lengths of the bone segments were collected from preoperative biplanar radiographs (EOS Imaging, Paris, France). Discretization of the model was done using fine mesh generation with tetrahedric elements that averaged 3 mm in size. This mesh was composed of 67,254 elements and 120,646 nodes (Fig. 2). The geometry of a posterior-stabilized TKA with fixed bearing was utilized using CAD software (SolidWorks, Dassault system, France).

2.2. Total knee arthroplasty implantation

The CAD software was then used to implant the TKA components (femoral component, tibial tray, tibial insert, polyethylene patellar dome component) using a mechanical alignment technique as follows: femoral and tibial bone cuts perpendicular to the femoral and tibial mechanical axes, respectively, 7° of femoral valgus, 3° of femoral external rotation, and 7° of tibial slope. The implantation was performed by a surgeon specialized in total joint replacement to optimize the size and position of the components based on the TKA implanted in the same patient *in vivo*. A 10-mm fixed bearing polyethylene tibial insert was inserted between the femoral and tibial components. Implants were rigidly fixed and kinematically constrained to their bone, with no modelling of the cement fixation.

2.3. Material properties

The ligament structures were simulated as wire bodies aiming to reproduce physiological behavior (element working in tension but not in compression). The ligament attachments were defined using the initial imaging and validated by the surgeon (Fig. 2). The bones and implants were considered as rigid deformable bodies with fully linked interfaces (except for the patellofemoral and tibiofemoral joints). Friction coefficients of $\mu = 0.02$ and $\mu = 0.05$ were applied to the patellofemoral and tibiofemoral joints, respectively [17]. The mechanical properties attributed to materials (Table 2) and soft tissues (Table 3) were assumed to be homogeneous and isotropic, and derived from the literature.

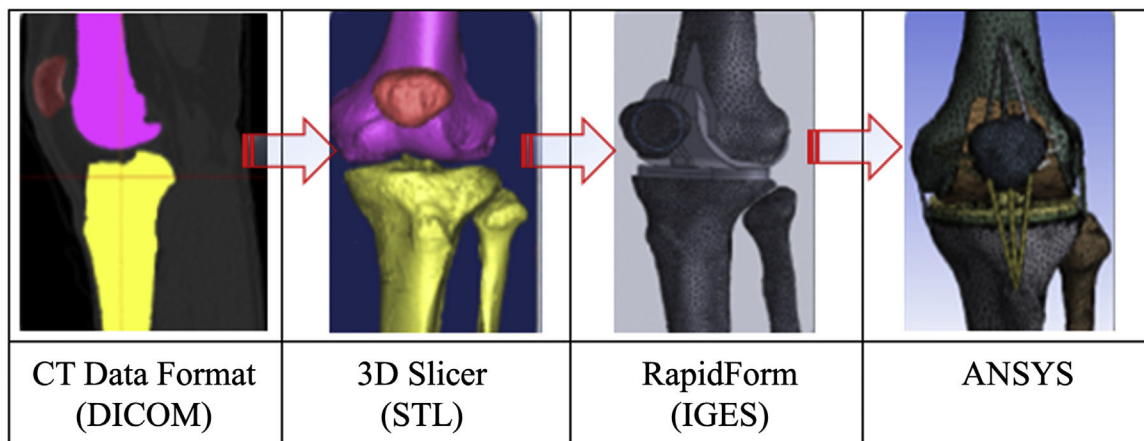


Fig. 1. Methodology using CT-scan for bone reconstruction and implant modeling.

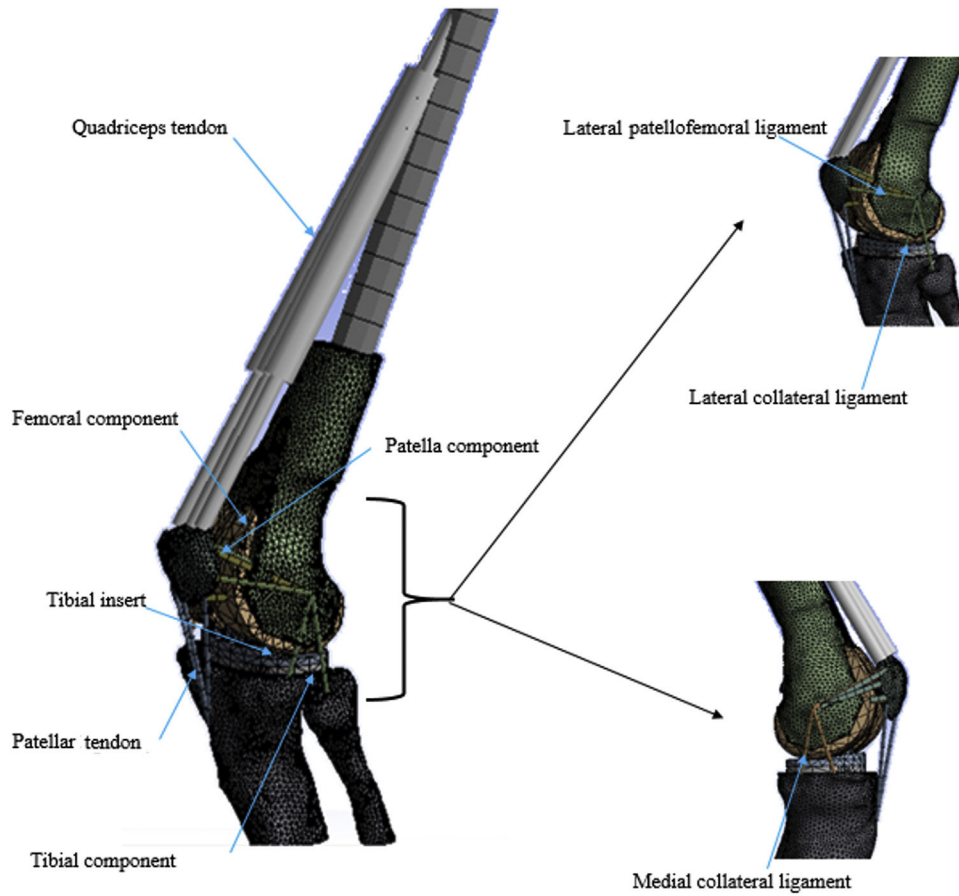


Fig. 2. Computational model of the total knee arthroplasty and the extensor mechanism using finite element analysis and mesh generation.

Table 2
TKA component properties.

Structure	Material	Young's Modulus E (MPa)	Poisson coefficient ν
Tibial insert, patellar implant	Polyethylene	685	0.4
Femoral implant	CrCoMo	220,000	0.3
Tibial implant	Titanium	110,000	0.3

Table 3
Ligament properties.

Structure	Young's modulus E (MPa)	Poisson coefficient ν	Surface (mm ²)
Lateral collateral ligament	180	0.4	9.42
Medial collateral ligament	160	0.4	9.42
Patellofemoral ligament	180	0.4	6.28
Patellar tendon	1600	0.4	9.42

2.4. Loading and boundary conditions

The Oxford Knee Rig setup [18], a well-controlled and reproducible experimental protocol, was reproduced *in silico*, while keeping the tibia fixed during flexion (Fig. 3). A constant 130 Newtons (N) load was applied to the center of the femoral head along an axis joining the centers of the femoral head and ankle, to simulate the loading conditions during a squatting motion while standing on both legs [17]. As such, the direction of force applied varied depending on the flexion angle, by inducing a flexion moment \vec{C} in the knee replacement (Fig. 3). The components F_x (along $\vec{x}0$) and F_y (along $\vec{y}0$) and the force \vec{F} and moment \vec{C} were determined using the following equations:

$$C = F \times d$$

$$d = L1 \times \sin \beta1$$

$$\theta = \beta1 + \beta2$$

$$d = L1 \times \sin (\theta - \beta2)$$

$$F_x = F \times \cos (\beta2) \text{ and } F_y = F \times \sin (\beta2)$$

The parameters F , d , $L1$, $\beta1$ and $\beta2$ were defined as shown in Fig. 4.

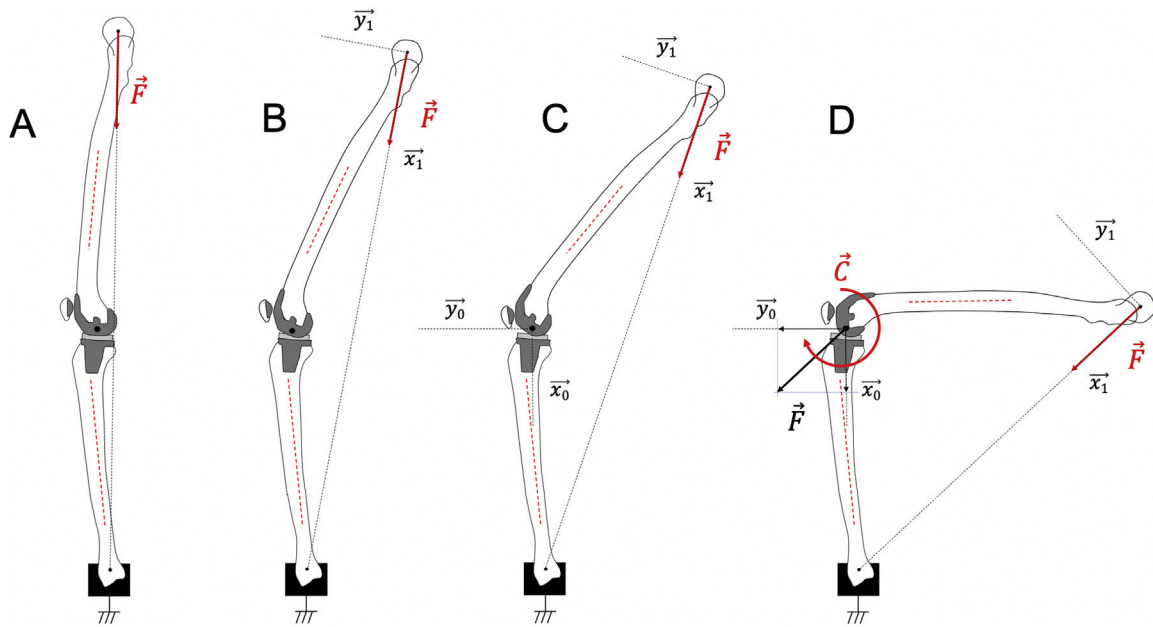


Fig. 3. Boundary conditions in the sagittal plane during a squat simulation. Initial load on the femoral head (A), expression of this load in the mobile femoral frame with flexion angle (B), definition of a new fixed knee frame (C), application of the initial load in the knee frame inducing a moment at the center of the knee replacement (D).

The quadriceps tendon was modeled using unidimensional viscoelastic elements (shocks and springs set in parallel). The damping coefficients were chosen to minimize dynamic effects. The action of the hamstring muscles was ignored during the flexion movement [10,19]. The analysis was completed for each flexion position (20°, 30°, 40°, 60°, 80°, 100°) after having first calculated the quadriceps stiffness, for which the knee was maintained in equilibrium due to external loads.

2.5. Validation study

The results were compared to experimental data (cadaver studies using the Oxford Knee Rig) or validated computer data with similar loading conditions. For a squatting motion, the comparability analysis used standardized forces of twice the load applied initially (noted $BW=2*130N=260\text{ N}$) as per Mason et al. [20]. The validation study included forces applied to the quadriceps tendon (F_Q) and patellar tendon (F_{PT}), contact forces (medially and laterally, and medial/lateral ratio) and contact pressure on the tibiofemoral joint, and the flexion angle at which post-cam contact occurred (defined by the flexion angle at which the contact force was no longer null during flexion).

2.6. Output data

Patellofemoral contact force (F_{PF} , expressed in N) and Von Mises stress on the patellar implant (expressed in MPa) were evaluated for each position in flexion.

3. Results

3.1. Quadriceps force

Quadriceps force increased continuously with knee flexion angle, reaching a maximum of about 6 times the applied load at 100° flexion (Fig. 5).

3.2. Patellar tendon force

The patellar tendon force F_{PT} /quadriceps force F_Q ratio was slightly reduced with increasing knee flexion angle (Fig. 6).

3.3. Tibiofemoral contact forces and pressure

Lateral and medial tibiofemoral contact forces increased continuously with knee flexion angle, up to 407 N medially and 257 N laterally at 100° flexion. The medial-to-lateral distribution on the tibial insert was 64% and 36%, respectively. The contact pressure map on the tibial insert relative to knee flexion angle showed peak contact pressure more posteriorly with flexion, with a femoral roll-back pattern (Fig. 7).

3.4. Post-cam contact forces

Post-cam contact forces started increasing slightly below 70° of knee flexion.

3.5. Patellofemoral contact forces and Von Mises stress (output data)

Patellofemoral contact forces F_{PF} increased from 20° to 100°, reaching 7 times the initial applied load (i.e. 3.5 times the BW value) (Fig. 8), and were correlated with increasing force applied to the quadriceps tendon (Fig. 9). The maximal F_{PF}/F_Q ratio was about 40% during our simulation. Von Mises stress on the patellar implant increased from 5.5 MPa (20° flexion) to 16.4 MPa (100° flexion) on average (Fig. 10). While they were initially centered, the stress shifted proximally and medially on the patellar implant, likely attributable to patellar contact with the intercondylar notch.

4. Discussion

The aim of this study was to validate a new finite element model of a TKA that provides reliable biomechanical data on the patellofemoral joint reaction forces during a simulated squatting motion. Finite element analysis is a method known for its precise

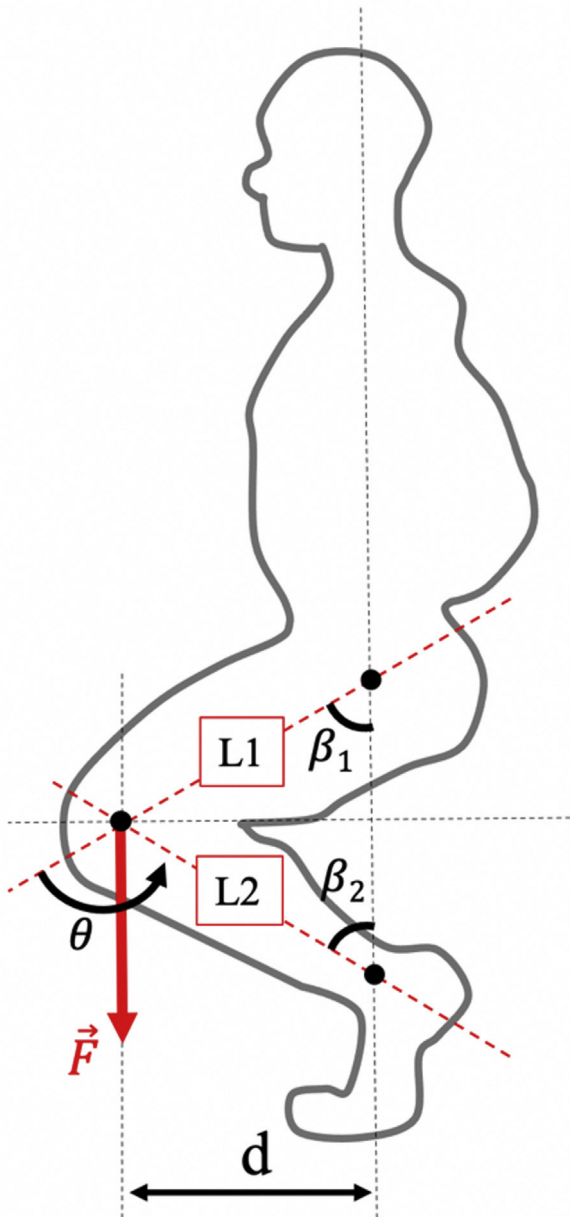


Fig. 4. Expression of the force \vec{F} in the sagittal plane during a squat activity.

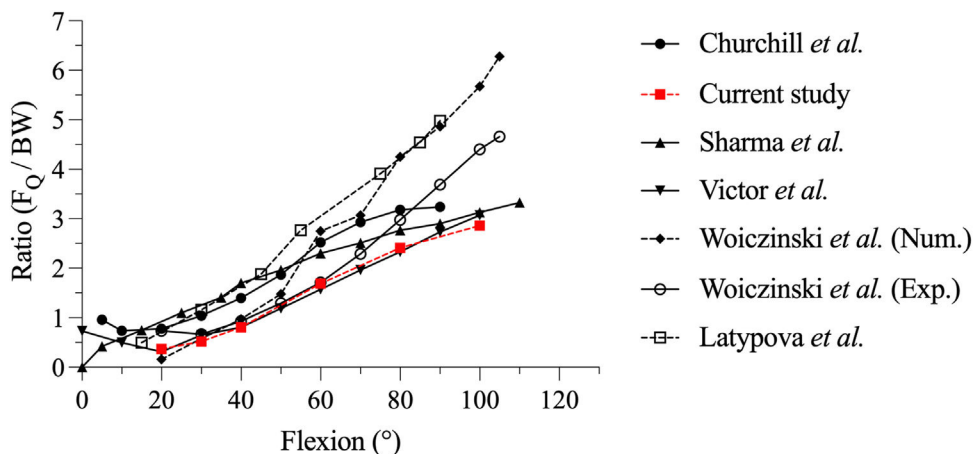


Fig. 5. Changes in quadriceps tendon force relative to body weight ($F_Q/BW=$) under squat loading conditions, compared to literature.

calculation of joint loads, generating mechanical output data related to deformable elements [21]. Thus, this is a reference method for understanding the forces exerted on the extensor mechanism during flexion.

The initial step of the computer validation focuses on the tibiofemoral joint's loads and kinematics, similar to the *in vivo* or experimental conditions observed after implantation of posterior-stabilized TKA: presence of posterior femoral roll-back of several millimeters without paradoxical anterior translation, limited lateral lift-off of femoral condyles during flexion [22,23]. In our simulation, the tibiofemoral contact forces, their distribution between the medial and lateral compartments (about 60% vs. 40%), along with the instant of post-cam contact (typically reported to be between 60° and 75° flexion) were consistent with several published studies [22,24,25].

The innovative method of our approach included an *a priori* calculation of the quadriceps stiffness to equilibrate the model at the given flexion angle. The 130 N applied load was similar to the loading conditions used by Victor et al. [23]. By standardizing external forces to twice the applied load, forces applied to the extensor mechanism were consistent with Victor et al. and other experimental studies in which external forces were determined by inverse kinematics [26,27]. Quadriceps force was 6 times higher than the initially applied load at 100° flexion, which is suitable for squatting motion [23]. However, a large variability of quadriceps force values exists in the literature, ranging from one to two times our results [11]. Previously collected kinematic tibiofemoral data from experimental study can be incorporated and used to drive the finite element simulation, which can over-estimate quadriceps force [28].

Patellofemoral contact force increased gradually during knee flexion and proportionally to the quadriceps force. Finally, the distribution pattern and magnitude of Von Mises stress on the patellar implant were comparable to the literature [26,27,29]. Interestingly, the highest mean Von Mises stress found in our simulation (16 MPa at 100° flexion) was similar to experimental results from Glaser et al. (17 MPa at 90° flexion), values surpassing the polyethylene yield point of the patellar implant (14.4 MPa) from 90° of flexion [30].

This study has some limitations. First, a single implant design was used, thus these results cannot be generalized to other TKA implants. Second, the validation analysis was restricted to published studies with comparable loading and boundary conditions. While two types of mesh were tested with no major impact on the results, conducting a numerical sensitivity analysis by changing the mesh or material parameters could enhance the validity of our model. Additionally, our simulation was designed to ana-

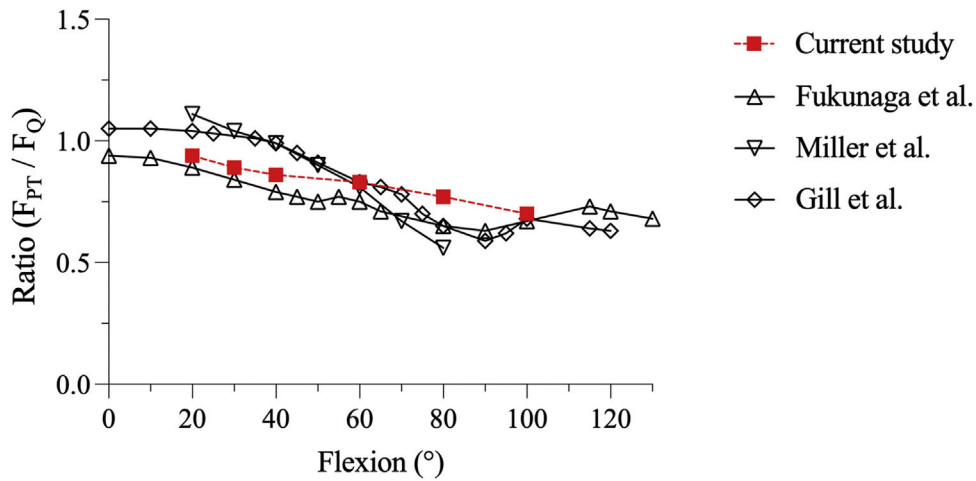


Fig. 6. Changes in patellar tendon force F_{PT} / quadriceps force F_Q ratio during flexion, compared to literature.

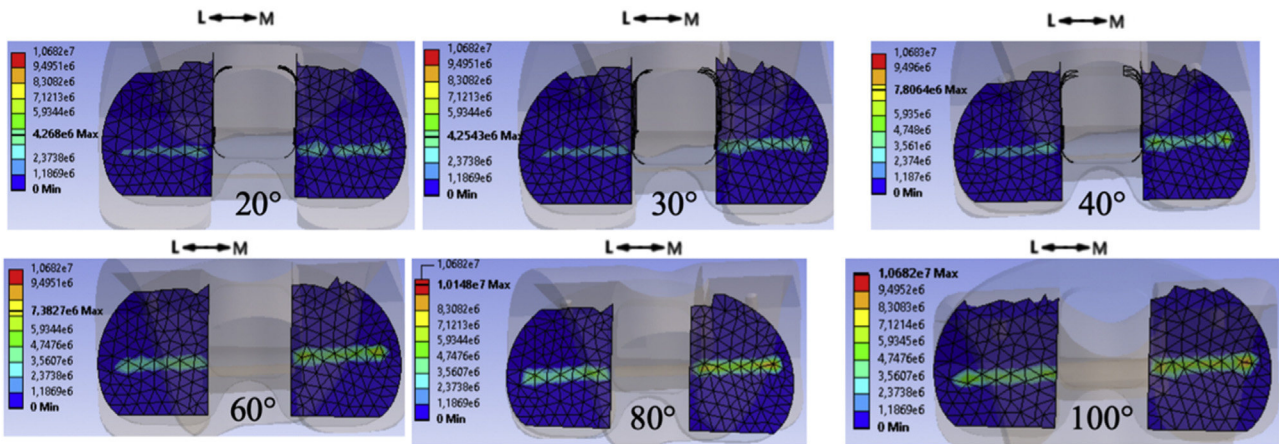


Fig. 7. Contact stress distribution on the tibial insert during flexion.

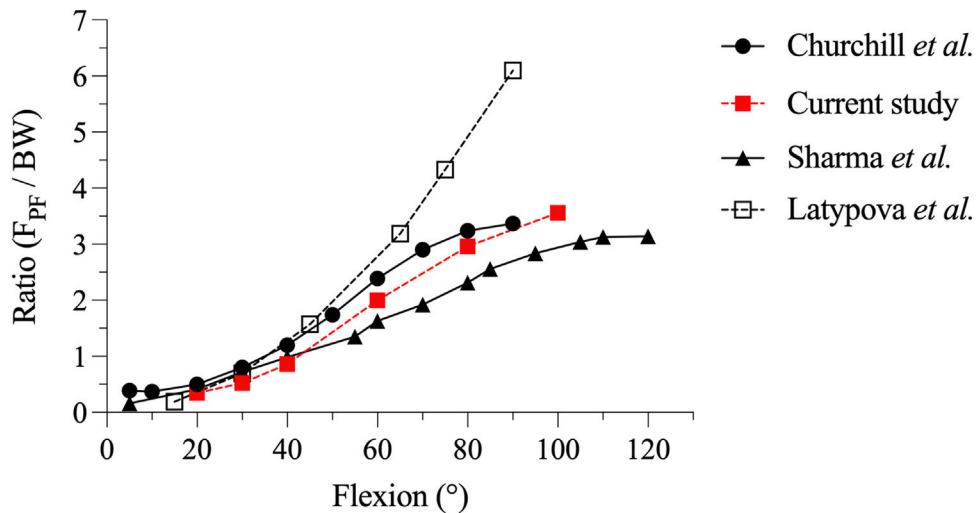


Fig. 8. Changes in patellofemoral contact forces relative to body weight (F_{PF}/BW) under squat loading conditions, compared to literature. BW = twice the load applied initially (260 N)

lyze extensor mechanism reaction forces and patellofemoral stress as output data, thus patellofemoral kinematics were not collected. Lastly, model inputs such as the patellar retinaculum [31,32], hamstring tendons [33] and more complex collateral ligaments models

[34] could be incorporated to provide more realistic patellofemoral behavior during squatting motion. In addition to some intraoperative tools [35], a preoperative computational simulation tool could predict individual patellofemoral forces and contact pressure with

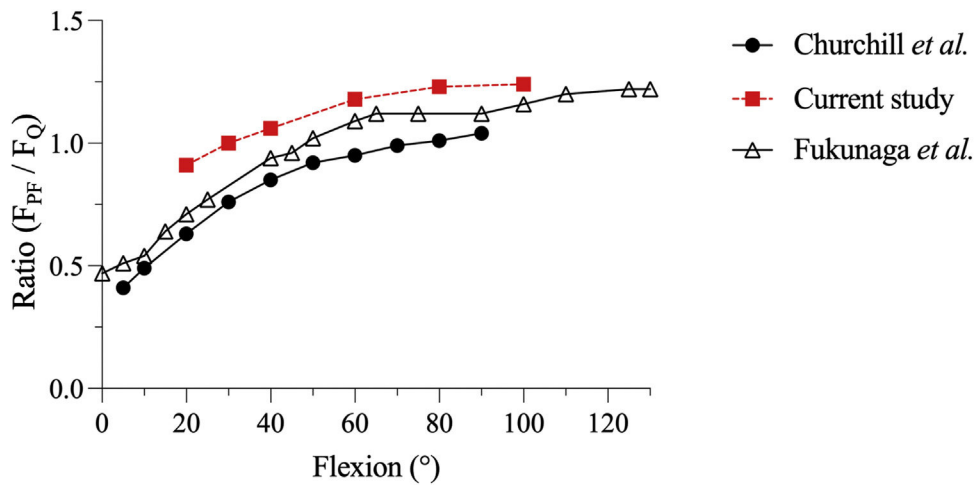


Fig. 9. Changes in patellofemoral contact force F_{PF} / quadriceps force F_Q ratio , compared to literature.

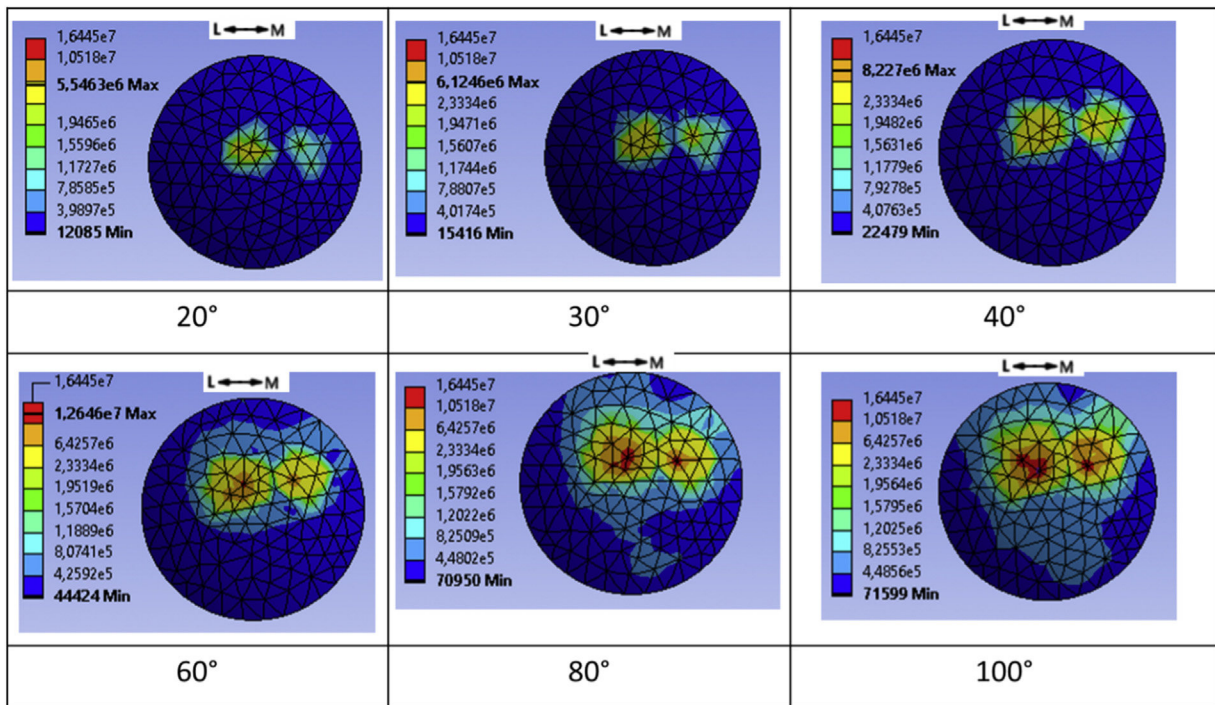


Fig. 10. Von Mises stress distribution in the patellar implant during flexion.

respect to implant position or patient-specific anatomy, providing data that would help the surgeon in planning the TKA implantation.

5. Conclusion

This study showed agreement among literature and our computational model for patellofemoral forces and stress under squatting conditions after TKA implantation. This model furthers our understanding of the influence of implantation techniques on patellofemoral reaction forces during flexion.

Disclosure of interest

The authors declare that they have no competing interest.

Funding

Agence Nationale de la Recherche (ANR): LabEx NuMEV Scholarship (SM).

Author contributions

L.D.: investigation, methodology, formal analysis, visualization, writing – original draft, writing – review and editing.

S.M.: investigation, methodology, computational analysis, visualization, writing–original draft, writing – review and editing.

E.M.: writing – review and editing.

F.C.: visualization, writing – review and editing.

F.J.: conceptualization, computational analysis, project administration, writing – review and editing.

References

- [1] Canovas F, Dagneaux L. Quality of life after total knee arthroplasty. *Orthop Traumatol Surg Res* 2018;104:S41–6.
- [2] Galea VP, Rojanasopondist P, Connelly JW, Bragdon CR, Huddleston JI 3rd, Ingelsrud LH, Malchau H, Troelsen A. Changes in Patient Satisfaction Following Total Joint Arthroplasty. *J Arthroplasty*. 2020;35(1):32–38. doi: 10.1016/j.arth.2019.08.018. Epub 2019 Aug 10. PMID: 31492454.
- [3] Dagneaux L, Jordan É, Michel E, Karl G, Bourlez J, Canovas F. Are modern knee outcomes scores appropriate for evaluating anterior knee pain and symptoms after total knee arthroplasty? *Orthop Traumatol Surg Res* 2022;103292.
- [4] Van Onsem S, Van Der Straeten C, Arnout N, Deprez P, Van Damme G, Victor J. A new prediction model for patient satisfaction after total knee arthroplasty. *J Arthroplasty* 2016;31:2660–7.e1.
- [5] Hoshi K, Watanabe G, Kurose Y, Tanaka R, Fujii J, Gamada K. Mobile-bearing insert used with total knee arthroplasty does not rotate on the tibial tray during a squatting activity: a cross-sectional study. *J Orthop Surg* 2020;15:114.
- [6] Mizu-uchi H, Colwell CW, Flores-Hernandez C, Fregly BJ, Matsuda S, D'Lima DD. Patient-specific computer model of dynamic squatting after total knee arthroplasty. *J Arthroplasty* 2015;30:870–4.
- [7] Huang C-H, Hsu L-I, Lin K-J, Chang T-K, Cheng C-K, Lu Y-C, et al. Patellofemoral kinematics during deep knee flexion after total knee replacement: a computational simulation. *Knee Surg Sports Traumatol Arthrosc* 2014;22:3047–53.
- [8] Latypova A, Taghizadeh E, Becce F, Büchler P, Jolles BM, Pioletti DP, et al. Patellar bone strain after total knee arthroplasty is correlated with bone mineral density and body mass index. *Med Eng Phys* 2019;68:17–24.
- [9] Latypova A, Arami A, Becce F, Jolles-Haerberli B, Aminian K, Pioletti DP, et al. A patient-specific model of total knee arthroplasty to estimate patellar strain: a case study. *Clin Biomech* 2016;32:212–9.
- [10] Bori E, Innocenti B. Development and validation of an in-silico virtual testing rig for analyzing total knee arthroplasty performance during passive deep flexion: a feasibility study. *Med Eng Phys* 2020;84:21–7.
- [11] Woiczinski M, Steinbrück A, Weber P, Müller PE, Jansson V, Schröder Ch. Development and validation of a weight-bearing finite element model for total knee replacement. *Comput Methods Biomech Biomed Engin* 2016;19:1033–45.
- [12] Baldwin MA, Clary CW, Fitzpatrick CK, Deacy JS, Maletsky LP, Rullkoetter PJ. Dynamic finite element knee simulation for evaluation of knee replacement mechanics. *J Biomech* 2012;45:474–83.
- [13] Innocenti B, Pianigiani S, Labey L, Victor J, Bellemans J. Contact forces in several TKA designs during squatting: a numerical sensitivity analysis. *J Biomech* 2011;44:1573–81.
- [14] Fitzpatrick CK, Rullkoetter PJ. Influence of patellofemoral articular geometry and material on mechanics of the unresurfaced patella. *J Biomech* 2012;45:1909–15.
- [15] Viceconti M, Olsen S, Nolte L-P, Burton K. Extracting clinically relevant data from finite element simulations. *Clin Biomech* 2005;20:451–4.
- [16] Erdemir A, Guess TM, Halloran J, Tadepalli SC, Morrison TM. Considerations for reporting finite element analysis studies in biomechanics. *J Biomech* 2012;45:625–33.
- [17] Huang C-H, Hsu L-I, Chang T-K, Chuang T-Y, Shih S-L, Lu Y-C, et al. Stress distribution of the patellofemoral joint in the anatomic V-shape and curved dome-shape femoral component: a comparison of resurfaced and unresurfaced patellae. *Knee Surg Sports Traumatol Arthrosc* 2017;25:263–71.
- [18] Bourne R, Goodfellow JW, O'Connor J. A functional analysis of various knee arthroplasties. *Trans Orthop Res Soc* 1978;24:160.
- [19] Victor J, Labey L, Wong P, Innocenti B, Bellemans J. The influence of muscle load on tibiofemoral knee kinematics. *J Orthop Res* 2009, <http://dx.doi.org/10.1002/jor.21019>.
- [20] Mason JJ, Leszko F, Johnson T, Komistek RD. Patellofemoral joint forces. *J Biomech* 2008;41:2337–48.
- [21] Bori E, Innocenti B. Development and validation of an in-silico virtual testing rig for analyzing total knee arthroplasty performance during passive deep flexion: a feasibility study. *Med Eng Phys* 2020;84:21–7.
- [22] Argenson J-NA, Scuderi GR, Komistek RD, Scott WN, Kelly MA, Aubaniac J-M. *In vivo* kinematic evaluation and design considerations related to high flexion in total knee arthroplasty. *J Biomech* 2005;38:277–84.
- [23] Belvedere C, Leardini A, Catani F, Pianigiani S, Innocenti B. *In vivo* kinematics of knee replacement during daily living activities: condylar and post-cam contact assessment by three-dimensional fluoroscopy and finite element analyses: contact assessment in total knee replacement. *J Orthop Res* 2017;35:1396–403.
- [24] Wang Y, Yan S, Zeng J, Zhang K. The biomechanical effect of different posterior tibial slopes on the tibiofemoral joint after posterior-stabilized total knee arthroplasty. *J Orthop Surg* 2020;15:320.
- [25] Innocenti B, Pianigiani S, Labey L, Victor J, Bellemans J. Contact forces in several TKA designs during squatting: a numerical sensitivity analysis. *J Biomech* 2008;41:642–8.
- [26] Sharma A, Leszko F, Komistek RD, Scuderi GR, Cates HE, Liu F. *In vivo* patellofemoral forces in high flexion total knee arthroplasty. *J Biomech* 2008;41:642–8.
- [27] Churchill DL, Incavo SJ, Johnson CC, Bynnon BD. The influence of femoral roll-back on patellofemoral contact loads in total knee arthroplasty. *J Arthroplasty* 2001;16:909–18.
- [28] Nakamura S, Tanaka Y, Kuriyama S, Nishitani K, Ito H, Furu M, et al. Superior-inferior position of patellar component affects patellofemoral kinematics and contact forces in computer simulation. *Clin Biomech* 2017;45:19–24.
- [29] Latypova A, Taghizadeh E, Becce F, Büchler P, Jolles BM, Pioletti DP, et al. Patellar bone strain after total knee arthroplasty is correlated with bone mineral density and body mass index. *Med Eng Phys* 2019;68:17–24.
- [30] Glaser FE, Gorab RS, Lee TQ. Edge loading of patellar components after total knee arthroplasty. *J Arthroplasty* 1999;14:493–9.
- [31] Wang J, Wang S, Yang Y, Guo D, Liu J, Chen X, et al. Effect of patellar tendon release on squatting characteristics of tibiofemoral joint after total knee arthroplasty: a simulation analysis. *Review* 2020, <http://dx.doi.org/10.21203/rs.3.rs-87075/v1>.
- [32] Koh Y-G, Son J, Kwon O-R, Kwon SK, Kang K-T. Effect of post-cam design for normal knee joint kinematic, ligament, and quadriceps force in patient-specific posterior-stabilized total knee arthroplasty by using finite element analysis. *BioMed Res Int* 2018;2018:1–11.
- [33] Stevens-Lapsley JE, Balter JE, Kohrt WM, Eckhoff DG. Quadriceps and hamstrings muscle dysfunction after total knee arthroplasty. *Clin Orthop* 2010;468:2460–8.
- [34] Naghibi Beidokhti H, Janssen D, van de Groes S, Hazrati J, Van den Boogaard T, Verdonschot N. The influence of ligament modelling strategies on the predictive capability of finite element models of the human knee joint. *J Biomech* 2017;65:1–11.
- [35] Ogawa H, Sengoku M, Shimokawa T, Nakamura Y, Ohnishi K, Matsumoto K, et al. Extra-articular factors of the femur and tibia affecting knee balance in mechanically aligned total knee arthroplasty. *Orthop Traumatol Surg Res* 2022;103297.